Supporting Information

Tuneable Hierarchical Self-Assembly of C_3-Symmetric Triaminoguanidium-derivative into Rhombic Dodecahedral Morphology

Ananta Dey,[a,b] Arunava Maity,[a] Tufan Singha Mahapatra,[a,c] Eingathodi Suresh,[a,b] Amal Kumar Mandal,[a,b] and Amitava Das*[a,b,d]*

[a] Analytical and Environmental Science Division and Centralized Instrument Facility,
CSIR-Central Salt and Marine Chemicals Research Institute,
Bhavnagar, Gujarat-364002, India.
E-mail: a.das@csmcri.res.in

[b] Academy of Scientific and Innovative Research (AcSIR),
CSIR- Human Resource Development Centre,
(CSIR-HRDC) Campus, Sector 19, Kamla Nehru Nagar,
Ghaziabad, Uttar Pradesh-201 002, India.

[c] ICFAI Science School (Chemistry),
ICFAI University Tripura,
Agartala-799210, Tripura (W), India.

[d] Department of Chemical Sciences
Indian Institute of Science Education and Research Kolkata,
Mohanpur, 741 246, West Bengal, India.
Email: amitava@iiserkol.ac.in

1. Materials and Characterization:

Materials: All the chemicals used for the synthesis of L purchased from Sigma-Aldrich Chem. Co. and were used as received without any further purification. All solvents were of reagent grade and procured from local companies. All solvents were dried and distilled before use by following standard procedures.

Characterization: Geol resonance ECZ600R spectrometer was used for ^{1}H NMR study. Agilent 6545 Q-TOF LC/MS instrument was used for mass spectroscopic measurement. Using a Shimadzu Corp 80109, UV-Vis spectrophotometer equipped with a Peltier system UV-Vis absorption spectra were measured. A Perkin Elmer 883 spectrometer was used for FT-IR spectroscopy using KBr pellets in the range oof 4000e cm^{-1} – 400 cm^{-1}. FE-SEM images were collected using a JEOL JSM-7100F instrument operated at an 18 kV accelerating voltage. An ultrathin coating of Au (~4 nm) was deposited via high vacuum evaporation. A Philips X'pert X-ray powder diffractometer using Cu-Kα radiation (l = 1.5418 Å) over a 2Θ range of 5–60 was used for recording the powder X-ray diffraction. Single crystal data was collected on a BRUKER SMART APEX (CCD) diffractometer equipped with a graphite monochromator and Mo-Ka radiation (l = 0.71073 Å) at 150 K. Using the SMART and SAINT software packages data collection and reduction were accomplished.[1] Multiscan empirical absorption corrections were applied to the data using the program SADABS.[2] The full-matrix least-squares technique was followed to solve the structure using SHELXTL and was refined on F2.[3] Crystallographic data (excluding structure factors) of L have been deposited in the Cambridge Crystallographic Data Centre as supplementary publications with CCDC no -1886920 and 1961480.

2. Synthesis of L:

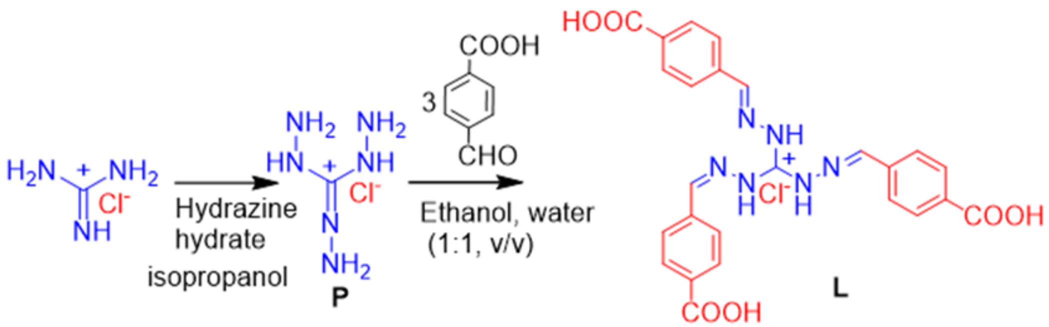

Figure S1: Synthesis route of L.

Synthesis of P: Triaminoguanidinium chloride was prepared by the literature method.[4]

Synthesis of L: Triaminoguanidinium chloride (0.5 gm, 3.5 mmol) and 4-formylbenzoic acid (1.5 gm, 10.6 mmol) were dissolve in a (1:1 v/v) ethanol/water mixture and stirred for 4h at 90 ^{o}C. After that, the resulting mixture was cooled to room temperature. After some time, a large amount of yellowish-white precipitate was obtained. The desired product was washed using ethanol and dried under reduced pressure. Yield 1.5 gm (82%). ^{1}H NMR (600 MHz, DMSO- d_6): δ ppm 8.75 (3H, s), 8.10-8.06 (12H, m). ^{13}C NMR (125 MHz, DMSO- d_6): 166.9, 150.6, 147.6, 138.0, 131.7, 129.5, 127.5. (FT - IR) (ν cm^{-1}): -C=N str. frequency (~1600.8 cm^{-1}), $\nu_{C=O}$ 1713.9 cm^{-1}, ν_{OH} 3477.4 cm^{-1}. HRMS: m/z calculated for $[M]^+$ $(C_{25}H_{21}N_9)^+$: 501.4785; found: 501.1594. Elemental analysis calculated for $C_{25}H_{21}ClNO_6$: C, 55.92; H, 3.94; N, 15.65. Found C, 55.90; H, 3.90; N, 15.63.

3. ^{1}H NMR & ^{13}C NMR spectrum of L:

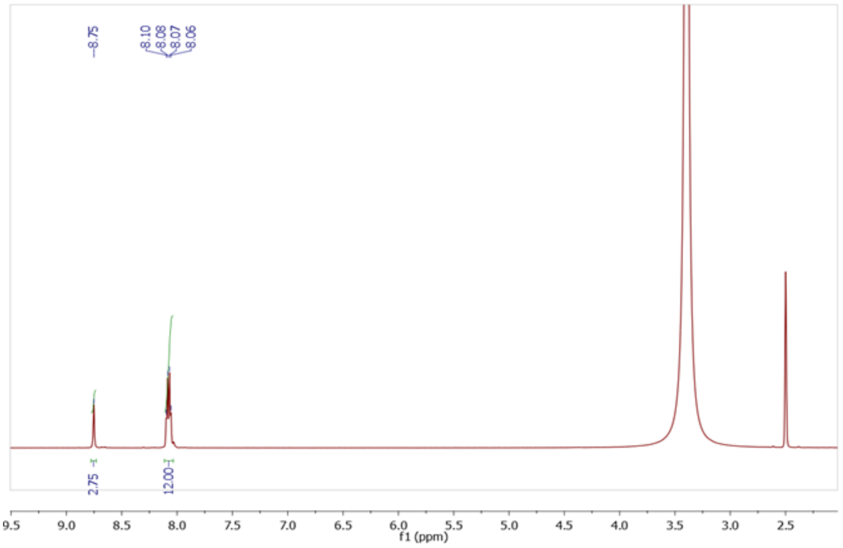

Figure S2: ^{1}H NMR spectrum of L recorded in DMSO-d_6.

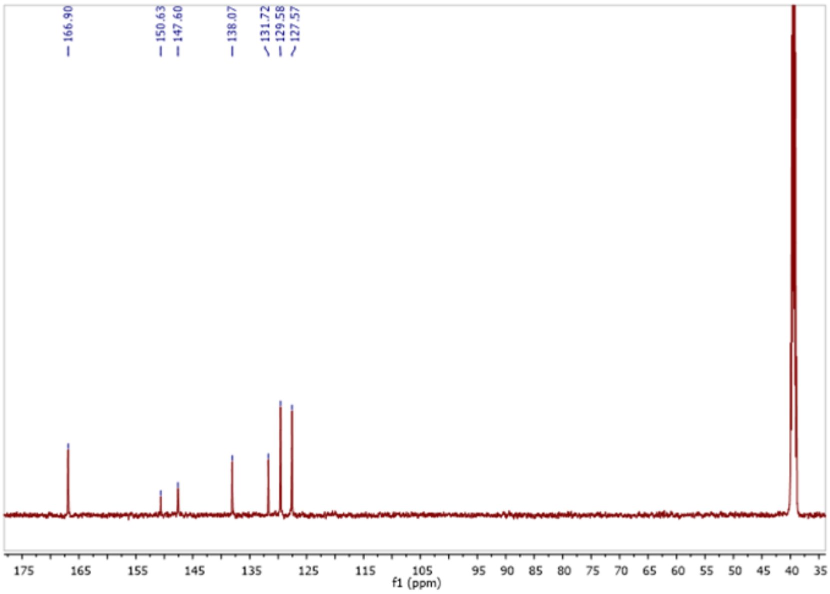

Figure S3: ^{13}C NMR spectrum of L recorded in DMSO-d_6.

4. HRMS & IR spectrum of L:

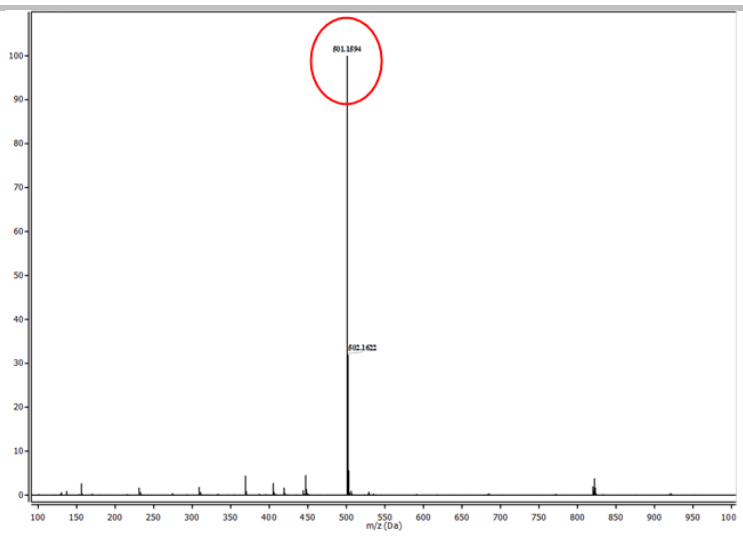

Figure S4: HRMS spectrum of L recorded in Methanol.

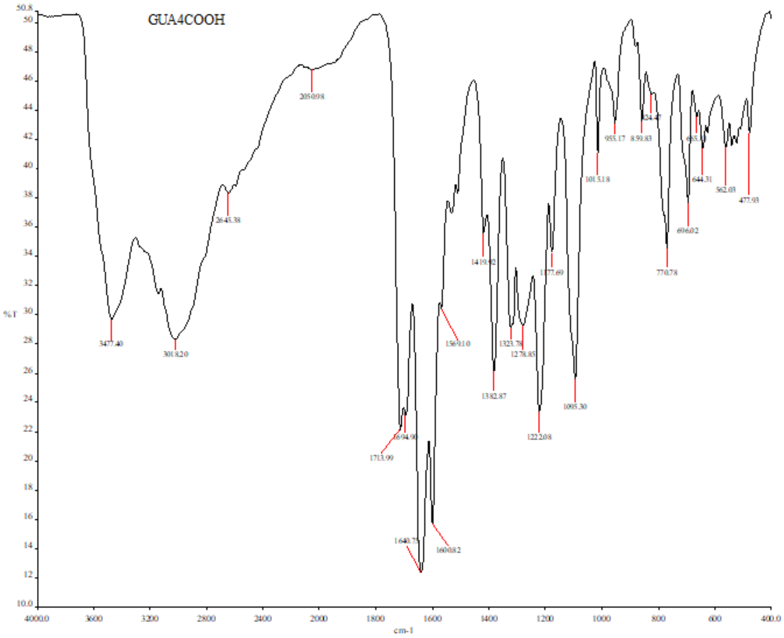

Figure S5: FT-IR spectrum of L recorded using KBr plate, -C=N str. frequency (~1600.8 cm^{-1}), $\nu_{C=O}$ 1713.9 cm^{-1}, ν_{OH} 3477.4 cm^{-1}.

5. Methods of sample preparation for FE-SEM:

The self-assembled microstructure and its formation mechanism were studied in DMSO/water and DMF/water solvent mixtures. First, a solution of L was prepared in pure DMSO with a concentration of 1mg/ml. 300 μL of this solution exposed to (2:1, v/v DMSO/water, 900 μL), (1:2 v/v DMSO/water, 900 μL), and 900 μL of water to prepare three different solutions of same effective concentration with the effective solvent composition of 3:1; 1:1 and 1:3 v/v DMSO/water. After vigorous shaking for one minute, the effective solutions were left undisturbed for about 10 minutes to stabilize. From that solution, 20 microlitre was drop-cast on Si (100). Finally, it was dried under a desiccator. Before taking images, samples were coated with gold vapor. Similarly, we prepared three different solutions of the same effective concentration with the solvent composition of 3:1; 1:1 and 1:3; v/v DMF/water, to study the self-assembly morphology in DMF/water solvent system.

6. FE-SEM images of L at 2.0 mg/mL concentration:

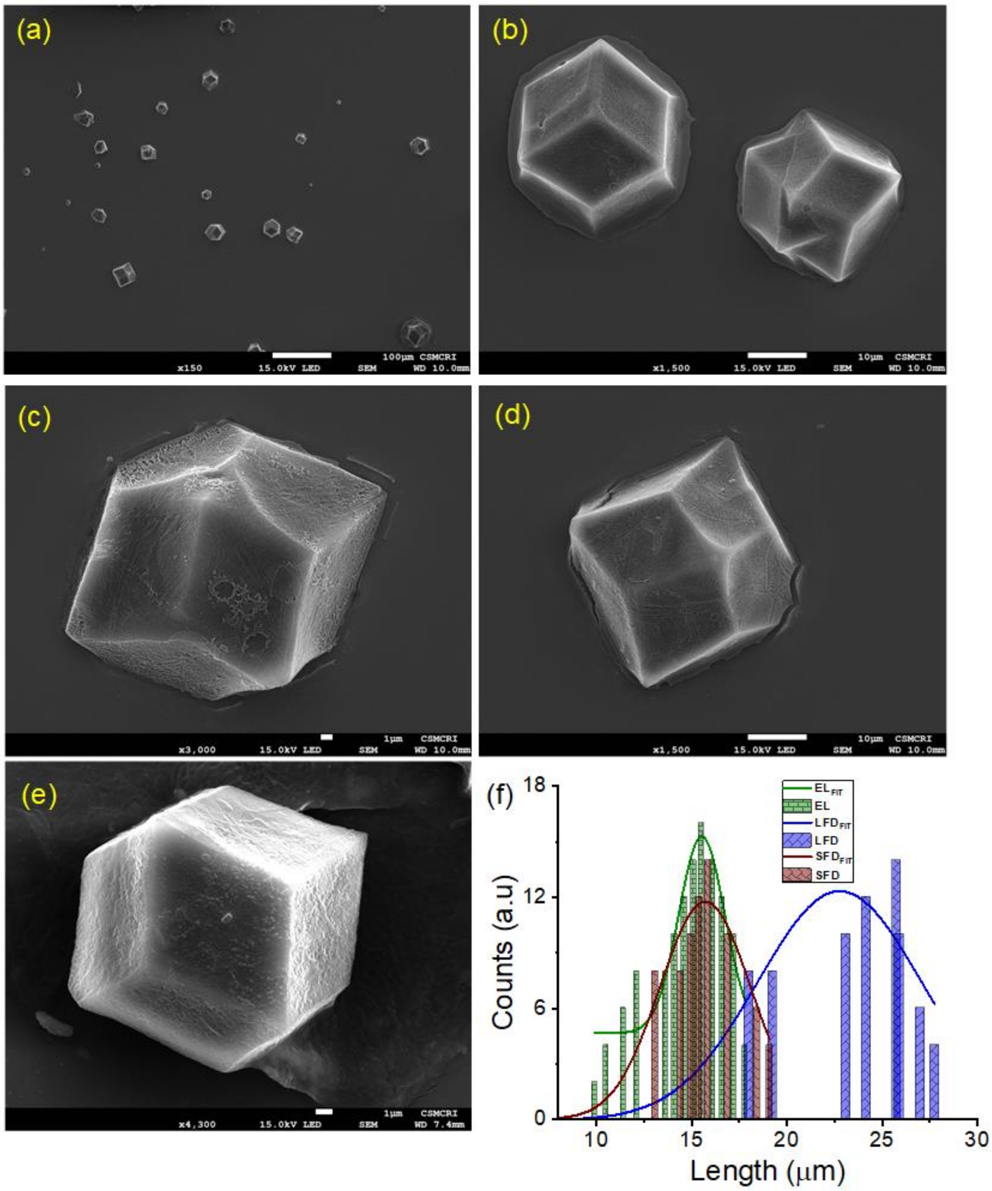

Figure S6: (a) – (e) FE-SEM image of self-assembled RD morphology of L, in DMSO/water (1:3 v/v) solvent system at a concentration of 2.0 mg/mL. (b) Statistical plot of length distribution histogram of RD morphology. LFD: blue bar; SFD: brown bar; EL: green bar, Solid line is the corresponding Gaussian fit. LFD: long face diagonal; SFD: short face diagonal; EL: edge length.

7. FE-SEM images of L at 0.5 mg/mL concentration:

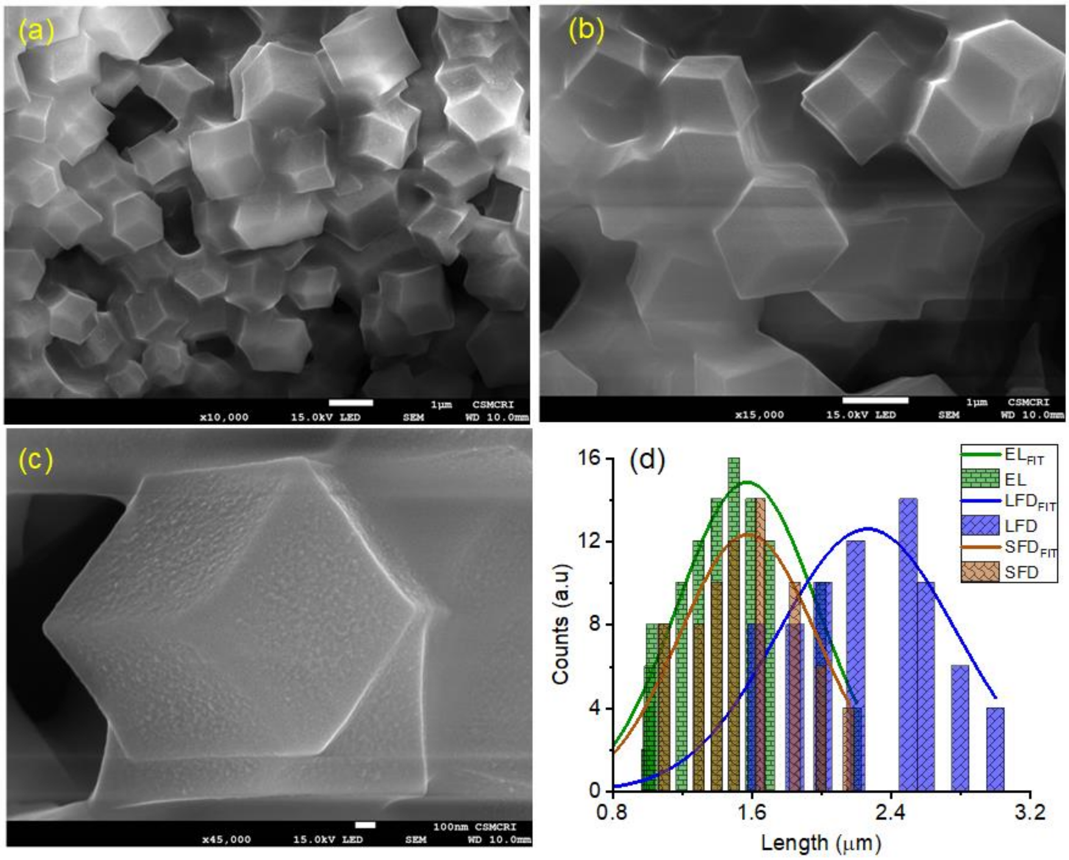

Figure S7: (a) – (e) FE-SEM image of self-assembled RD morphology of L, in DMSO/water (1:3 v/v) solvent system at a concentration of 0.5 mg/mL. (b) Statistical plot of length distribution histogram of RD morphology. LFD: blue bar; SFD: brown bar; EL: green bar, Solid line is the corresponding Gaussian fit. LFD: long face diagonal; SFD: short face diagonal; EL: edge length.

8. Determination of the degree of aggregation (α_{agg}):

The degree of aggregation (α_{agg}) was calculated from the temperature-dependent UV-Vis spectral data by using the equation (1) as mentioned bellow.

$$\alpha\ (T) = \frac{\varepsilon\ (T) - \varepsilon_M}{\varepsilon_A - \varepsilon_M}\ldots\ldots\ldots\ldots\ldots\ldots\ldots\ldots\ldots\ldots\ldots\ldots(1)$$

Where $\varepsilon(T)$ is the measured extinction coefficient at temperature T; ε_M and ε_A are the extinction coefficients of the monomer and fully aggregated state, respectively. The latter two values determined from the spectral data at high and low temperatures, respectively.

The experimentally determined degree of aggregation was fitted temperature-dependent isodesmic self-assembly model accordingly with equation (2) as mentioned below to obtain the enthalpy value ΔH.

$$\alpha(T) = \frac{1}{1+\exp[-0.908\Delta H\frac{T-T_m}{RT_m^2}]}\ldots\ldots\ldots\ldots\ldots\ldots\ (2)$$

Where α is the degree of aggregation, and T_m is the melting temperature was defined as the temperature at $\alpha = 0.5$ at $T = T_m$. R is the Boltzmann constant.

From the experimentally determined degree of aggregation, the number-averaged degree of polymerization, DP_N, calculated temperature-dependent isodesmic self-assembly model accordingly with equation (3), as mentioned below.

$$DP_N(T) = \frac{1}{\sqrt{1-\alpha(T)}} \dots\dots\dots\dots\dots\dots\dots\dots. (3)$$

From the number-averaged degree of polymerization, DP_N, and the known concentration of molecules, c_T, the equilibrium constant K_e was determined as a function of temperature using equation (4) as mentioned below.

$$DP_N(T) = \frac{1}{2} + \frac{1}{2}\sqrt{4K_e(T)C_T + 1} \quad \dots\dots\dots\dots\dots\dots\dots\dots (4)$$

9. UV-Vis spectral data in DMSO/water solvent:

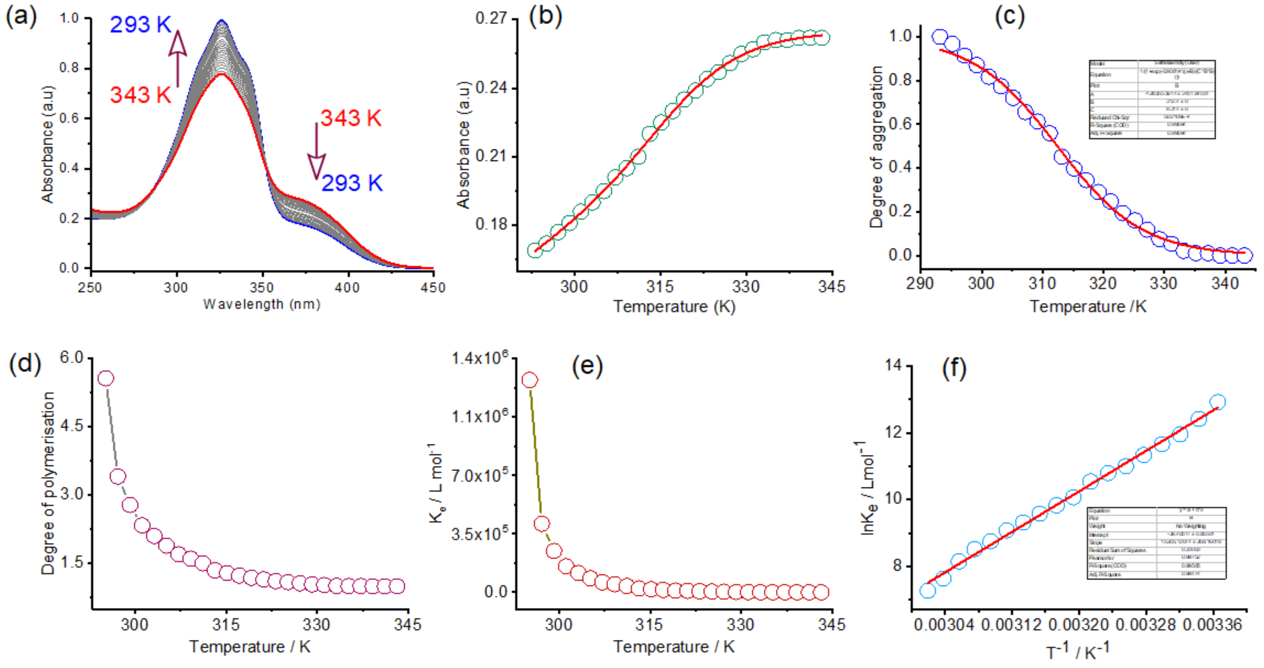

Figure S8: (a) Variable temperature UV-Vis spectra of L (1.0 × 10^{-5} M) in DMSO/water (1:3 v/v). (b) Corresponding plot of change of absorbance at 377 nm with temperature. (c) Temperature-dependent degree of aggregation, calculated from UV-Vis spectral change at 377 nm and corresponding isodesmic fit. (d) Corresponding plot of the degree of polymerization, DP_N, as a function of temperature. (e) Corresponding plot of the equilibrium constant, K_e, as a function of temperature. (f) Corresponding Van't Hoff plot for L in DMSO/water (1:3 v/v).

10. Crystal data in DMSO/water solvent:

60 mg of compound L was dissolved in 3 mL of DMSO and taken in a screw-capped vial. After that, 100 microliter water was added. The solution was gently heated, then kept it in a 10 ml beaker with no

mechanical disturbance for allowing the crystals of L to grow. After ~two weeks of high-quality rod-shaped yellow coloured crystals were obtained, which was used for X-ray diffraction.

Table S1. Parameters and refinement data for crystal L1, a DMSO hydrate of composition $(C_{25}H_{21}N_6O_6)$ + •$2(C_2H_6O_S)$•Cl•H_2O, obtained from DMSO/water solvent.

Compound reference	L1
Chemical formula	$C_{29}H_{35}ClN_6O_9S_2$
Formula Mass	711.20
Crystal system	Triclinic
Space group	$P\bar{1}$
Crystal color	Colourless
Crystal size/mm^3	0.34×0.19×0.18
a/Å	10.3837(18)
b/Å	11.2946(19)
c/Å	15.743(3)
$\alpha/^o$	88.521(3)
$\beta/^o$	89.943(3)
$\gamma/^o$	68.863(3)
V/Å^3	1721.5(5)
Z	2
D_c/g cm^{-3}	1.372
μ (mm^{-1})	0.291
F(000)	744
$T/^oK$	150(2)
Total reflns	13415
R(int)	0.0363
Unique reflns	6678
Observed reflns $(I > 2\sigma(I))$	4796
Parameters	516
R_1 $(I > 2\sigma(I))$ wR_2(all reflns)	0.0634, 0.1578
GOF (F^2)	1.034

CCDC number	1886920

$R_1 = \Sigma(||F_o|-|F_c||)/\Sigma|F_o|$. $wR_2 = [\Sigma w(|F_o|-|F_c|)^2/\Sigma w(F_o)^2]^{1/2}$. $w = 0.75/(\sigma^2(F_o) + 0.0010F_o^2)$

Table S2. Details of hydrogen bonding interactions observed in the crystal structure of L1 and L2.

D-H···A	d(H···A) (Å)	d(D···A) (Å)	∠D-H···A (°)
L1			
N1-H1D···Cl1^{1}	2.60(3)	3.281(3)	147(3)
N3-H3D···O7^{2}	2.12(4)	2.834(4)	155(3)
O9-H9E···Cl1^{3}	2.36(5)	3.158(3)	162(5)
O2-H2C···O9^{4}	1.78(4)	2.585(4)	167(4)
O3-H3C···Cl1^{5}	2.27(5)	3.015(3)	159(4)
O5-H5C···O8^{6}	1.86(4)	2.643(4)	173(4)
O9-H9F···O8^{7}	2.02(5)	2.786(4)	170(4)
C10-H10···O7^{5}	2.45(3)	3.185(4)	139(3)
C24-H24···O4^{8}	2.58(3)	3.378(4)	154(3)
C26-H26A···O4^{7}	2.56	3.516(5)	166
C26-H26B···O8^{3}	2.56	3.327(5)	135
C27-H27B···O6^{6}	2.49	3.357(6)	147
Symmetry code : 1. 1-x,-y,1-z; 2. -1+x,y,z; 3.x,y,z; 4. x,-1+y,1+z; 5. -1+x,y,z 6; -x,2-y,2-z; 7. 1-x,1-y,1-z; 8. x,y,1+z			
L2			
N1-H1···O7 ^{1}	2.07	2.882(4)	152
O3-H3C ···O9^{2}	1.73(5)	2.560(5)	168(5)
O5-H5C···O8^{3}	1.78(5)	2.617(5)	158(5)
N5-H5D···Cl1^{4}	2.42(4)	3.268(4)	154(3)
C16-H16···Cl1^{4}	2.66	3.543(4)	155
C18-H18···Cl1^{4}	2.64(4)	3.490(5)	140(3)
C33-H33C···Cl1^{5}	2.72(6)	3.549(6)	135(4)
N3-H3D ···Cl1^{6}	2.54(5)	3.301(4)	143(4)
O2-H2C···Cl1^{7}	2.23(6)	3.010(4)	169(4)
C2 -H2 ···O7^{1}	2.41(4)	3.125(6)	135(3
C12-H12···O9^{6}	2.55(4)	3.407(6)	159(3)
C13-13···O3^{8}	2.58(4)	3.367(6)	144(4)
C24-H24···O1^{4}	2.56(4)	3.532(6)	173(3)
C27-H27A···O9^{7}	2.36(4)	3.348(6)	153(3)
C31-H31 ···O4^{9}	2.40(5)	3.328(6)	157(4)
C32-H32A···O1^{7}	2.55(6)	3.411(7)	141(4)
C32-H32C···O8 ^{10}	2.48(5)	3.470(8)	177(3)
Symmetry code : 1. x,1/2-y,1/2+z; 2. -x,1/2+y,-1/2-z; 3. 1-x,1-y,2-z;4. -x,1/2+y,1/2-z; 5. 1+x,y,z; 6. x,1/2-y,-1/2+z; 7.x, y,z; 8. -1-x,1-y,-1-z; 9. -x,-1/2+y,1/2-z; 10. x,y,-1+z			

11. Packing and H-bonding interactions of L1 and L2:

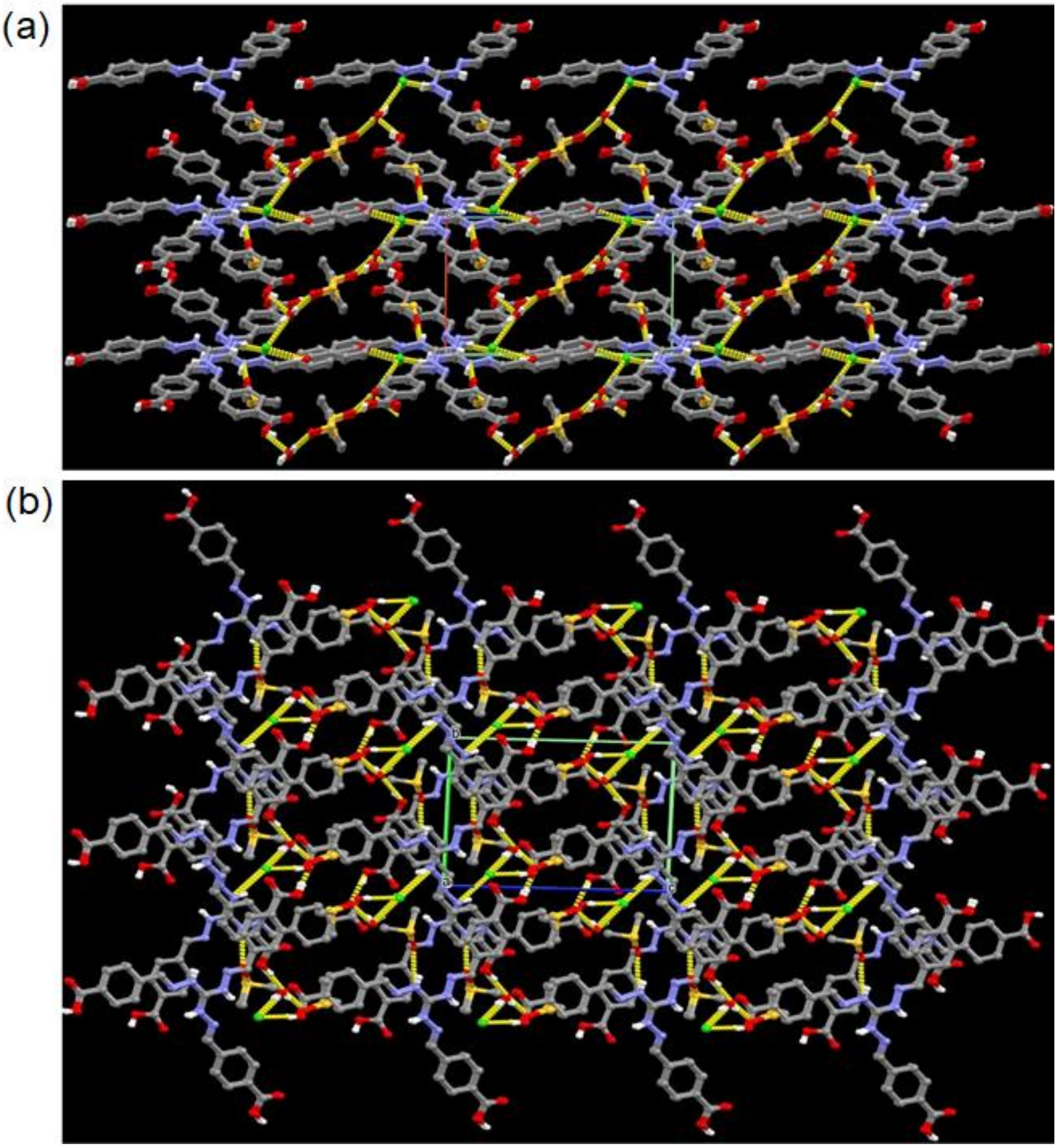

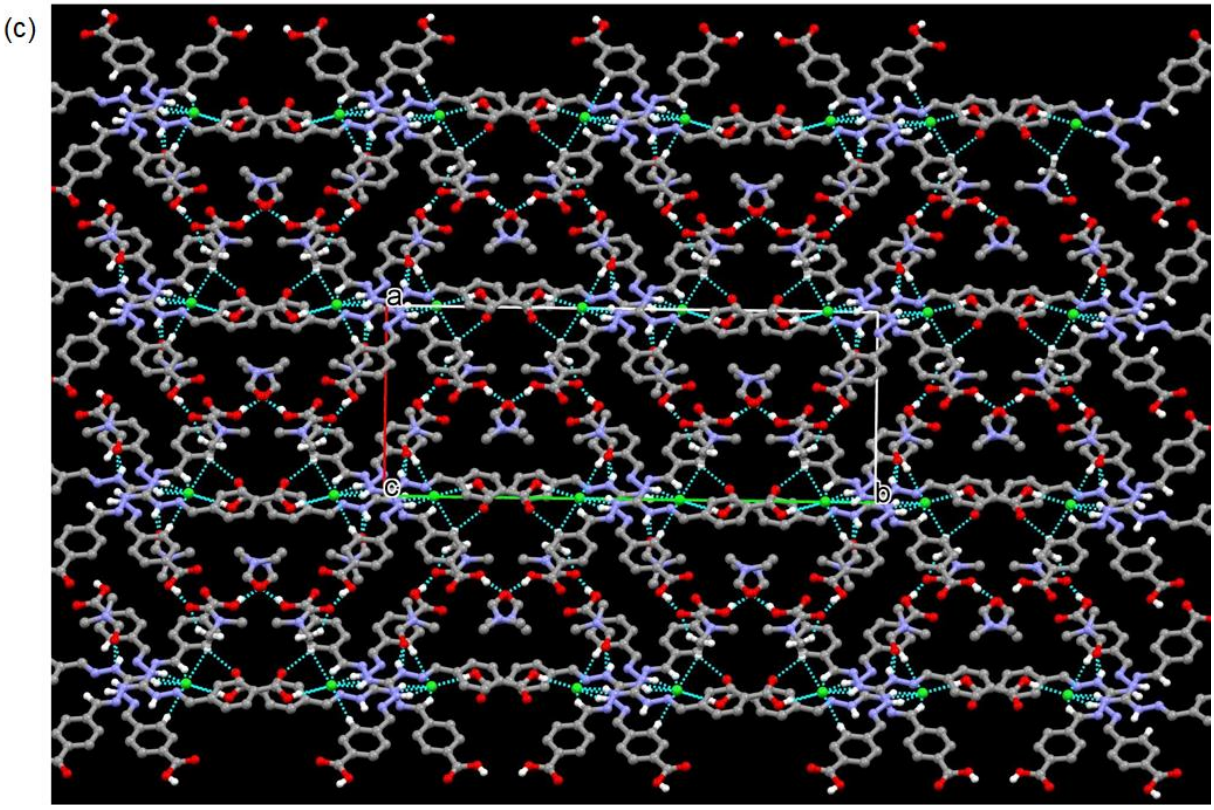

Figure S9: (a) Packing diagram with various hydrogen bonding interaction generating a 2D supramolecular network viewed down b-axis for crystal structure L1 grown in DMSO/water solvent system; (b) Packing diagram viewed down a-axis with various hydrogen bonding interaction generating a 2D supramolecular network viewed down a-axis for crystal structure L1 grown in DMSO/water solvent system. (c) Packing and H-bonding interaction viewed down the c-axis in depicting the supramolecular H-bonded network in L2 grown in DMF/water solvent system.

12. PXRD pattern of L in DMSO/water:

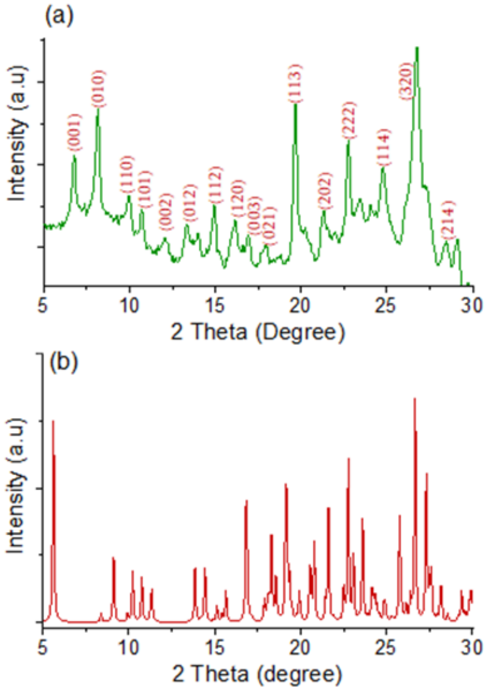

Figure S10: Wide-angle powder X-ray diffraction pattern recorded on (a) sedimentation of the self-assembled materials of L in DMSO/water (1:3 v/v); (b) Simulated XRD pattern obtained from the single crystal data.

13. FE-SEM image of L in DMSO/water (3:1 v/v):

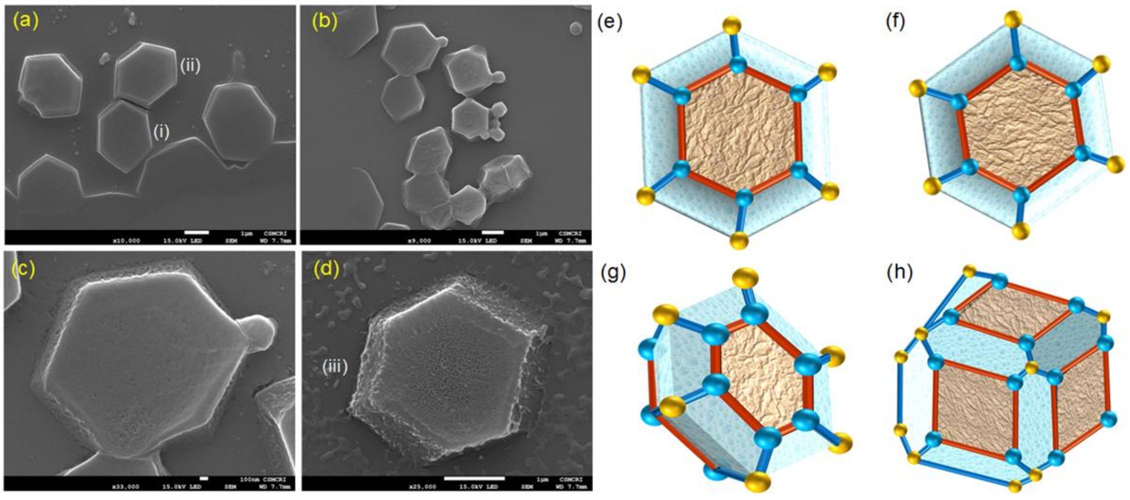

Figure S11: (a) – (d) FE-SEM image of self-assembled edge truncated triclinic morphology of L in DMSO/water (3:1 v/v) at a concentration of 1.0 mg/mL. Schematic representation of edge truncated triclinic morphology of their corresponding FE-SEM images (e) marked as (i); (f) marked as (ii); (g) marked as (iii) and edge truncated triclinic morphology with two distinct facets.

14. FE-SEM image of L in DMSO/water (1:1 v/v):

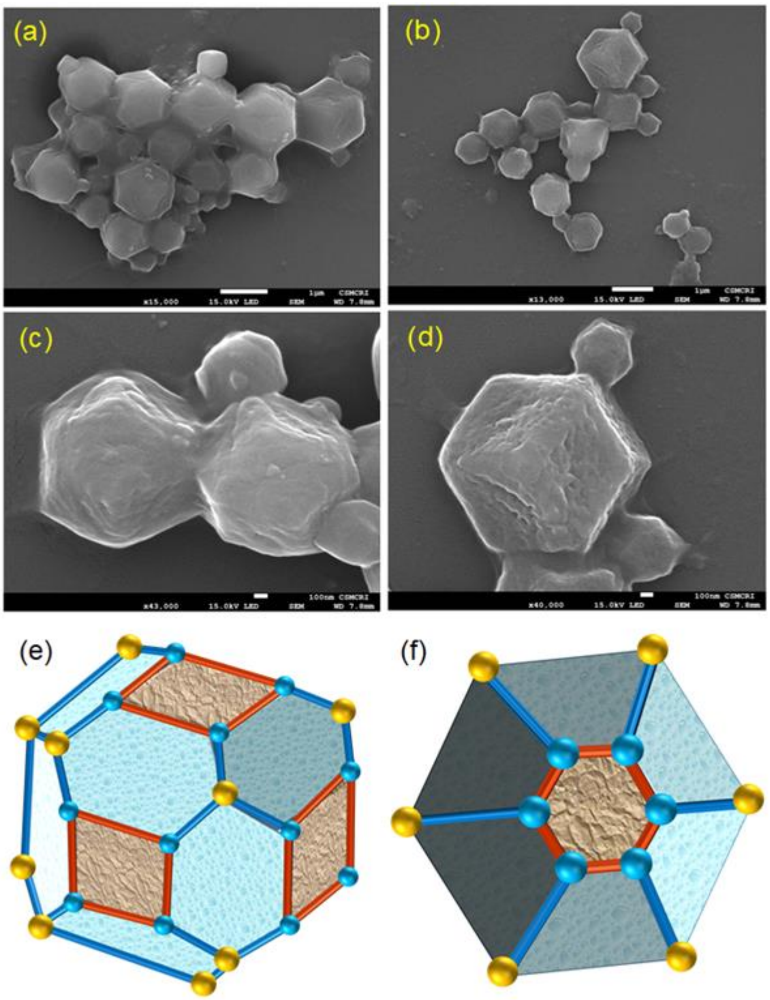

Figure S12: (a) – (d) FE-SEM image of self-assembled rhombi truncated triclinic morphology of L in DMSO/water (1:1 v/v) at a concentration of 1.0 mg/mL. Schematic representation of rhombi truncated triclinic morphology of their corresponding FE-SEM images with two distinct facets.

15. UV-Vis spectral data in DMF/water solvent:

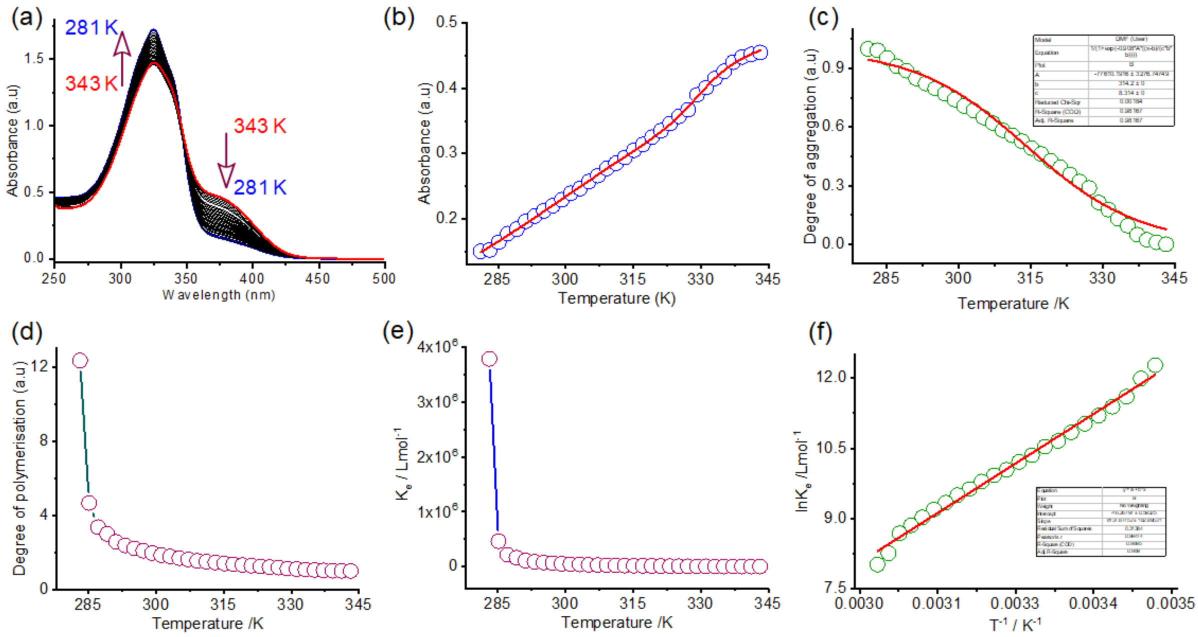

Figure S13: (a) Variable temperature UV-Vis spectra of L (3.7×10^{-5} M) in DMF/water (1:3 v/v). (b) Corresponding plot of change of absorbance at 377 nm with temperature. (c) Temperature-dependent degree of aggregation, calculated from UV-Vis spectral change at 377 nm and corresponding isodesmic fit. (d) Corresponding plot of the degree of polymerization, DP_N, as a function of temperature. (e) Corresponding plot of the equilibrium constant, K_e, as a function of temperature. (f) Corresponding Van't Hoff plot for L in DMF/water (1:3 v/v).

16. Crystal data in DMF/water solvent:

60 mg of compound L was dissolved in 3 mL of DMF and taken in a screw-capped vial. After that, 100 microliter water was added. The solution was gently heated, then kept it in a 10 ml beaker with no mechanical disturbance for allowing the crystals of L to grow. After ~two to three weeks of high quality, yellow coloured crystals were obtained, which was used for X-ray diffraction.

Table S3. Parameters and refinement data for crystal L2, a DMF solvate of composition $(C_{25}H_{21}N_6O_6)^{+}\bullet 3(C_3H_7NO)\bullet Cl$, obtained from DMF/water solvent.

Compound reference	L2
Chemical formula	$C_{34}H_{42}ClN_9O_9$
Formula Mass	756.22
Crystal system	Monoclinic
Space group	*P*2$_1$/*c*

Crystal color	yellow
Crystal size/mm^3	0.161 X 0.093 X 0.032
a/Å	12.625(2)
b/Å	32.160(6)
c/Å	9.2409(17)
α/^{o}	90
β/^{o}	95.599(4)
γ/^{o}	90
V/Å^3	3734.1(12)
Z	4
D_x/g cm^{-3}	1.345
μ (mm^{-1})	0.168
F(000)	1592
T/^{o}K	150(2)
Total reflns	18607
R(int)	0.0863
Unique reflns	6556
Observed reflns ($I > 2\sigma(I)$)	4188
Parameters	634
R_1 ($I > 2\sigma(I)$)	0.0946
wR_2(all reflns)	0.1700
GOF (F^2)	1.152
CCDC number	1961480

$R_1 = \Sigma(||F_o|-|F_c||)/\Sigma|F_o|$. $wR_2 = [\Sigma w(|F_o|-|F_c|)^2/\Sigma w(F_o)^2]^{1/2}$. $w = 0.75/(\sigma^2(F_o) + 0.0010F_o^2)$

17. PXRD pattern of L in DMF/water:

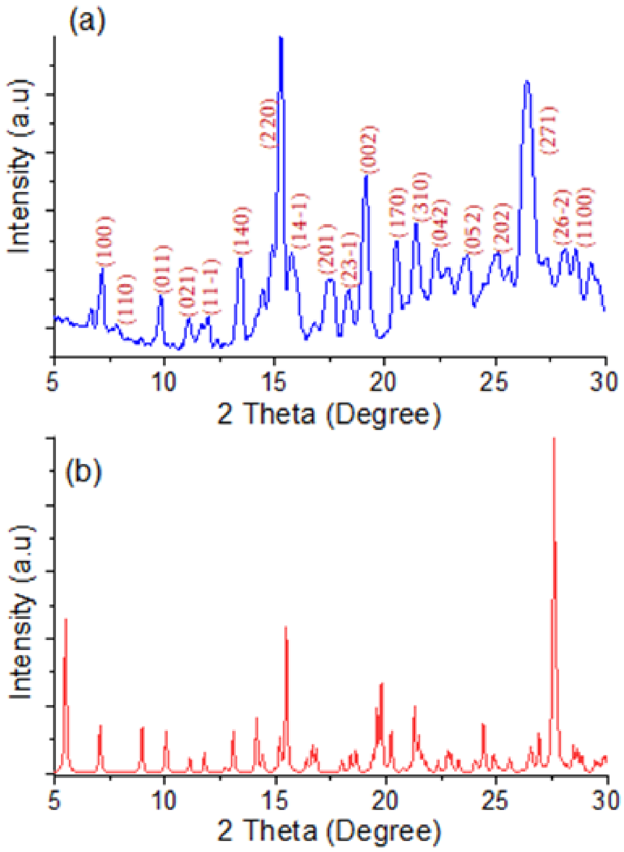

Figure S14: Wide-angle powder X-ray diffraction pattern recorded on (a) sedimentation of the self-assembled materials of L in DMF/water (1:3 v/v); (b) Simulated XRD pattern obtained from the single crystal data.

References:

(1) G. M. Sheldrick, SAINT 5.1 ed., Siemens Industrial Automation Inc., Madison, WI, 1995.

(2) SADABS, Empirical Absorption Correction Program, University of Go ¨ttingen, Go ¨ttingen, Germany, 1997

(3) G. M. Sheldrick, SHELXTL Reference Manual: Version 5.1, Bruker AXS, Madison, WI, 1997

(4) A. Maity, M. Gangopadhyay, A. Basu, S. Aute, S. S. Babu, and A. Das, *J. Am. Chem. Soc.* 2016, **138**, 11113–11116.